

Article

Evidence for Mild Diagenesis in Archaeological Human Bones from the Fewet Necropolis (SW Libya): New Insights and Implications from ATR–FTIR Spectroscopy

Francesca Castorina ^{1,2,*}, Umberto Masi ², Elisabetta Giorgini ^{3,*} , Lucia Mori ⁴ , Mary Anne Tafuri ⁵ and Valentina Notarstefano ³ 

¹ Dipartimento di Scienze della Terra, Università di Roma “La Sapienza”, Piazzale Aldo Moro 5, 00185 Roma, Italy

² CNR, IGAG c/o Dipartimento di Scienze della Terra, Università di Roma “La Sapienza”, Piazzale Aldo Moro 5, 00185 Roma, Italy

³ Dipartimento di Scienze della Vita e dell’Ambiente, Università Politecnica delle Marche, Via Breccie Bianche, 60131 Ancona, Italy

⁴ Dipartimento Scienze dell’Antichità, Università di Roma “La Sapienza”, Piazzale Aldo Moro 5, 00185 Roma, Italy

⁵ Dipartimento di Biologia Ambientale, Università di Roma “La Sapienza”, Piazzale Aldo Moro 5, 00185 Roma, Italy

* Correspondence: francesca.castorina@uniroma1.it (F.C.); e.giorgini@staff.univpm.it (E.G.)

Abstract: Bones offer a great amount of information on ancient populations regarding both their lifestyle habits and the influence of the living area. Bones are composed by an inorganic component, i.e., carbonated hydroxyapatite ($\text{Ca}_{10}[(\text{PO}_4)_6 - x(\text{CO}_3)_x](\text{OH})_2$), and an organic matrix (mainly proteins and collagen). After death, bones are subjected to diagenetic processes, with changes in structure, morphology, and chemical composition. All these modifications strictly depend on several factors, including the nearby environment, the climate, and the burial modality. Hence, a precise knowledge of the diagenetic processes affecting bones after death is mandatory. In this study, archaeological human bones from the Garamantian necropolis of Fewet (Libyan Sahara) were analyzed by ATR–FTIR spectroscopy to elucidate the role of the burial location and modality, as well as the highly arid environment in the diagenesis rate. Several spectral parameters related to structural and chemical features of the organic and mineral components (i.e., AmideI/PO₄, C/P, MM, FWHM₆₀₃, and IRSF indexes) were statistically analyzed. Spectral data were compared with those from modern ruminants from the same site to evaluate a possible time-dependent correlation between the chemical composition and the diagenetic processes. A mild diagenesis was found in all human bones, even though it had a variable degree depending on the burial location.

Keywords: ATR–FTIR spectroscopy; archaeological human bones; diagenesis; Fewet oasis; Garamantian necropolis; Libyan Sahara



Citation: Castorina, F.; Masi, U.; Giorgini, E.; Mori, L.; Tafuri, M.A.; Notarstefano, V. Evidence for Mild Diagenesis in Archaeological Human Bones from the Fewet Necropolis (SW Libya): New Insights and Implications from ATR–FTIR Spectroscopy. *Appl. Sci.* **2023**, *13*, 687. <https://doi.org/10.3390/app13020687>

Academic Editor: Giuseppe Lazzara

Received: 9 December 2022

Revised: 30 December 2022

Accepted: 31 December 2022

Published: 4 January 2023



Copyright: © 2023 by the authors. Licensee MDPI, Basel, Switzerland. This article is an open access article distributed under the terms and conditions of the Creative Commons Attribution (CC BY) license (<https://creativecommons.org/licenses/by/4.0/>).

1. Introduction

Bones are complex biological systems containing information at many different levels (i.e., isotopic, molecular, biochemical, and structural). They are mainly composed of bioapatite crystals consisting of inorganic nanosized crystallites of hydroxyapatite, $\text{Ca}_5(\text{PO}_4)_3(\text{OH})$, that are closely intertwined with an organic matrix composed by type I collagen and proteins [1]. After death, bones are subjected to modifications in terms of structure, morphology, and chemical composition; in general, the organic matrix is degraded, while the biomineral component undergoes a transformation to a more crystalline status, with the substitution of hydroxyl (OH[−]) or phosphate (PO₄^{3−}) groups with (CO₃)^{2−} ions (type A and B carbonated hydroxyapatite, respectively) and the replacement

of Ca^{2+} with other cations [1–3]. These alterations, which are also triggered by the environmental conditions and addressed as diagenesis, depend on several factors, including the uptake of cations, ions' exchange, degradation and leaching of collagen, microbiological attack, alteration, and, in some cases, leaching of the mineral matrix, infilling with mineral deposits, etc. [4–6].

The precise evaluations of the extent of diagenesis in archaeological bones is crucial for the reliable use of specific parameters, such as the chemical and isotopic composition, for studies regarding the diet and provenance of ancient populations [7]. In fact, diagenesis is not only concerned with the changes taking place in bones during burial, but it is also related to how the environment affects these changes to alter specific information [8].

Attenuated total reflectance-Fourier transform infrared (ATR-FTIR) spectroscopy is a quick, cost-effective, and non-destructive technique that is useful for studying the chemical and structural features of solid samples, including bones and teeth, which cannot be analyzed in transmission mode, since the radiation cannot pass through [9–12]. This technique obtains qualitative and quantitative information at a molecular level, not only regarding the mineral component, but also the organic matrix [10]. ATR-FTIR spectroscopy relies on the use of high refractive index crystals, such as diamonds and germaniums, within which the IR radiation can propagate as an internal reflection [13]. Even if the radiation is quite completely refracted by the surface of the sample, an evanescent wave is generated, which penetrates the sample and generates the corresponding IR spectrum. ATR-FTIR presents several advantages with respect to other conventional methods; in fact, it works independent of the sample type or thickness, and, therefore, a broad variety of materials can be measured [14]. The average spatial resolution of this technique is in the range of 100 μm , which is not high compared to other molecular spectroscopic techniques [15]. As an example, it has been used to assess postmortem changes in the bioapatite crystals (by analyzing specific spectral parameters, such as IRSF, FWHM₆₀₃, C/P, and MM) and in the organic matrix, by evaluating the amount of proteins with respect to inorganic phosphates [5,10,16,17].

The oasis of Fewet is located along the upper course of Wadi Tanezzuft, about 1200 km south of Tripoli and SE to Hammada El-Hamra in the Fezzan, which is next to the border between Libya and Algeria. The geomorphological description of the area has already been reported [18,19]. Excavations in the Fewet oasis revealed a rural village with a necropolis dated to the Garamantian time (3rd century B.C.–2nd century A.D.) [20], which represents one of the oldest settlements in SW Fezzan. This necropolis covers an area of approximately 150 hectares [21] and is set on the plateau located E to S of the Fewet village (Figure 1) hosting the Hasawnah Formation. This latter region, which is the oldest (Upper Cambrian) and most important by extent formation of the area, is composed of fluvial and deltaic conglomerates and sandstones, which are overhung by intertidal–subtidal silty and fine-grained materials, and covered by subtidal massive sandstones [22]. The necropolis hosts 1329 tumuli of conical to transitional and drum-shaped types; the tumuli contain human skeletons and/or dismembered bones in stone cists, which are occasionally infilled with loose sand, encircled by sandstone blocks/slabs, covered by a stony slab, and placed in shallow burial pits dug into the sandstone bedrock. In some tumuli, a few-centimeters thick, coarse reddish soil/sand occurs between the cist and the underlying bedrock. Some studies already reported in the literature regarding the human bones collected in this necropolis [23,24], but the impact of diagenesis on these samples is still poorly defined. Di Lernia et al. analyzed the carbon and nitrogen stable isotopes of those bones and gave only a few reliable results because of the impact of the hyper-arid climatic conditions [25]. Conversely, a Sr isotopic study performed on human tooth enamel from the same area provided information on the humans' diet and provenance [26].

In the light of this evidence, this present study aims to improve the knowledge on the diagenetic processes affecting these archeological remains in relation to the burial location and modality, as well as the highly arid environment. To this end, specific spectral parameters related to the structural and chemical features of the organic and inorganic com-

ponents (such as the Amide I/PO₄, C/P, MM FWHM₆₀₃, and IRSF indexes) were obtained by ATR–FTIR spectroscopy and statistically analyzed. Spectral data were compared with those of modern ruminants from the same site to evaluate a time-dependent correlation between the chemical composition and diagenesis. Moreover, spectral data of human bones from the Fewet oasis were compared with those reported in the literature regarding coeval humans inhumated in the Meroitic Al-Khiday cemetery (Sudan).

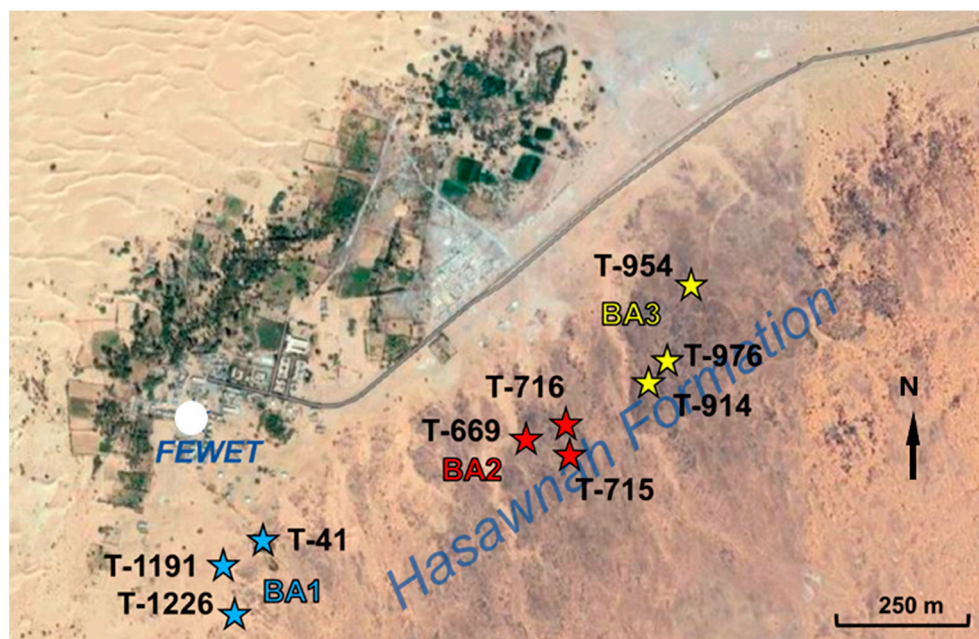


Figure 1. Satellite image of the Fewet oasis area in the Sahara of SW Libya (modified from Google maps), showing the three burial areas of the necropolis and the tumuli from which human bone samples were collected. Light blue stars: tumuli in BA1; red stars: tumuli in BA2; yellow stars: tumuli in BA3; white circle: Fewet village’s main settlement.

2. Materials and Methods

2.1. Samples Collection

Human bone samples were collected from 9 tumuli in the Garamantian necropolis of the Fewet oasis (Libyan Sahara). The necropolis can be divided into three burial areas: a flat lower area located in the SW of the Wadi Takarkori valley (named BA1); a central area with a gentle slope (name BA2), and a flat upper area located in the NE of the Fewet plateau (named BA3). Figure 1 shows the location of the tumuli within these areas: tumuli T-41, T-1191, and T-1226 are in BA1; tumuli T-669, T-715, and T-716 are in BA2, and tumuli T-914, T-954, and T-976 are in BA3. More specifically, all the tumuli were placed on a flat bedrock and the results were well-built, except for the tumuli T-41, T-1191, T-1226 (in BA1), and T-954 (in BA3), which were characterized by deflation and sanding over [23].

Portions of human (H) bones (mainly limb, rib, and fibula) were collected from the skeletons of 9 adult individuals (5 males, M, and 4 females, F); all the information regarding these samples is reported in Table 1 [24]. Samples H-41M, H-669F, H-715F, H-914F, H-954F, H-976M, and H-1191M showed a good state of preservation and completeness; conversely, the main anatomical parts of skeleton H-716M were poorly preserved, and, lastly, the skeleton H-1226M exhibited a very low degree of preservation and anatomical completeness.

In addition, 3 bone samples belonging to modern ruminants (2 jaws of Ovis/Capra, named A-2, A-6, and 1 pelvis fragment of a gazelle, named A-106) were retrieved from the Fewet village (named ENV) for comparative analysis with the archaeological human remains.

Table 1. Main features of the archaeological human bone samples collected in the Garamantian necropolis of the Fewet oasis in the Sahara of SW Libya (* From archaeological material—C14 date rejected) [24].

Sample	Sex	Maximum Age at Death	Bone	Conservation	Skeleton	Period	Burial Area	Topographic Location
H-41	M	30–35	rib	very good	complete	Classic/Late *	BA1	On the sandstone plateau
H-669	F	20–25	limb	very good	complete	Mature	BA2	On the slope of the sandstone plateau
H-715	F	20–25	rib	very good	complete	Classic	BA2	Flat area on the top of the sandstone plateau
H-716	M	20–30	limb	bad	incomplete	Late	BA2	On the sandstone plateau
H-914	F	15–20	limb	very good	complete	Classic	BA3	On the top of the sandstone plateau
H-954	F	20–25	limb	very good	complete	Mature	BA3	On the top of the sandstone plateau
H-976	M	35–40	fibula	very good	complete	Classic	BA3	Flat area on the top on the sandstone plateau
H-1191	M	25–30	fibula	very good	almost complete	Mature	BA1	Flat sandy area at the foot of the sandstone plateau
H-1226	M	40–45	limb	bad	incomplete	Mature	BA1	Flat sandy area at the foot of the sandstone plateau

2.2. ATR–FTIR Analysis

ATR–FTIR measurements were carried out by using a PerkinElmer Spectrum GX1 spectrometer (PerkinElmer, Inc., Waltham, MA, USA) equipped with a UATR accessory; a diamond/ZnSe crystal was used for analysis in reflectance mode.

The following procedure was applied to each sample. First, the external surface of the bone was gently cleansed with abrasive paper to eliminate soil sediments; then, five representative portions (ca. 10 mg) were collected and finely hand-ground in an agate mortar to obtain a homogeneous powder. The powder of each portion was deposited onto the surface of the diamond/ZnSe crystal, and the ATR–FTIR spectrum was acquired in reflectance mode in the 4000–450 cm^{-1} spectral range (64 scans, spectral resolution 4 cm^{-1}). A background spectrum was acquired before each sample acquisition.

For each bone sample, the absorbance average spectrum and the absorbance average spectra \pm S.D. spectra were generated by averaging the IR spectra collected on the five different portions (averaging routine, OPUS 7.5 software package, Bruker Optics, Ettlingen, Germany). The obtained average IR spectra were interpolated in the 1800–500 cm^{-1} spectral region, multi-point-baseline linear fitted, and vector normalized. To resolve convoluted bands and highlight underlying peaks, IR spectra were then curve fitted with Gaussian functions in the same spectral range. The position (expressed as wavenumbers) of each underlying peak was identified based on second derivative analysis and fixed before running the iterative process to obtain the best reconstructed curve (residual close to zero; bandwidth in 10 to 40 cm^{-1} range); this fitting procedure made it possible to calculate the exact area, height, and width of each underlying peak (GRAMS/AI 9.1, Galactic Industries, Inc., Salem, NH, USA) [27,28].

2.3. Statistical Analysis

IR data were first submitted to principal component analysis (PCA; OriginPro 2018b software, OriginLab Corporation, Northampton, MA, USA). Then, univariate analysis was performed by means of a factorial analysis of variance (one-way ANOVA), followed by Tukey’s multiple comparison test (statistical difference was set at $p < 0.05$; Prism6, Graphpad software, Inc., San Diego, CA, USA). IR data were also submitted to a linear regression to

monitor the relationship between the C/P and MM indexes (OriginPro 2018b software). Finally, a multinomial logistic regression was carried out to investigate both the real and numerical correlation between chemical bone composition and the following categorical dependent variables: (i) presumptive age of death (<30 years = 0, ≥ 30 years = 1), (ii) sex (male = 0, female = 1), (iii) chronological attribution (Classic = 0, Late = 1, Mature = 2), and (iv) burial areas (BA1 = 0, BA2 = 1, BA3 = 2, ENV = 3) (OriginPro 2018b software).

3. Results

The representative ATR–FTIR spectrum of a human bone sample collected in the Garamantian necropolis of the Fewet village and dated ~200 B.C.–~200 A.D., is reported as an example in Figure 2. The spectrum is shown in the 1800–450 cm^{-1} range, containing the most relevant spectral features attributable to hydroxyapatite; the bands were assigned according to the literature [3,5,16]. In particular, the peaks related to carbonate (centered at 1463 cm^{-1} , 1412 cm^{-1} , and 872 cm^{-1}), and phosphate (centered at 1091 cm^{-1} , 1024 cm^{-1} , 956 cm^{-1} , 603 cm^{-1} , and 565 cm^{-1}) groups in carbonated hydroxyapatite were well evident; in addition, a band referring to the organic component (proteins and collagen) was detected at 1639 cm^{-1} . It is noteworthy that no peak at 712 cm^{-1} attributable to diagenetic calcite was found in any of the bone samples.

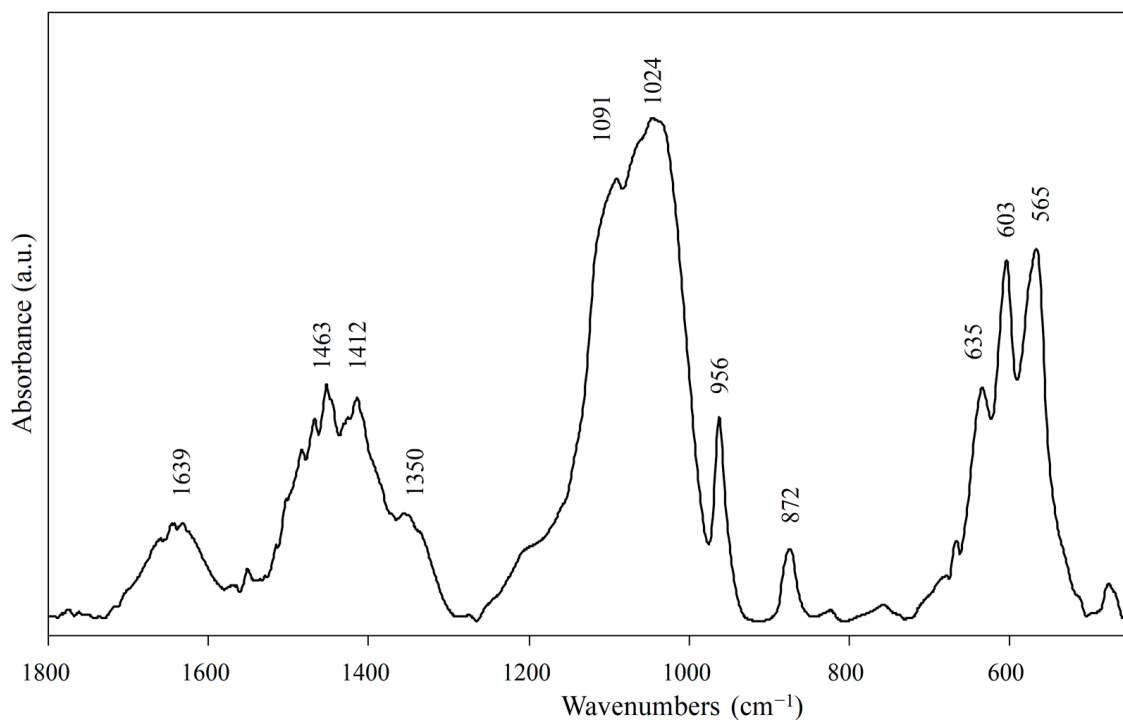


Figure 2. ATR–FTIR spectrum of a representative human bone sample from the Fewet oasis in the Sahara of SW Libya. The spectrum is displayed in the 1800–500 cm^{-1} region; the positions of the most relevant peaks (in terms of wavenumbers, cm^{-1}) are reported for clarity.

The ATR–FTIR spectra of all bone samples analyzed (human and animal) were used to calculate the following diagenetic spectral parameters: IRSF (infrared splitting factor, calculated by dividing the sum of the intensity of the peaks at 603 cm^{-1} and 565 cm^{-1} and the intensity of the valley between them), which is related to bioapatite crystallinity [5,17,29]; FWHM_{603} (full width at half maximum of the band centered at 603 cm^{-1}), which is inversely proportional to the mineral crystallinity index and representative of the apatite phosphate environment [16]; C/P index (calculated as the ratio between the intensities of the peaks at 1412 cm^{-1} and 1024 cm^{-1} attributed to vibrational modes of carbonate and phosphate groups, respectively), which is related to the carbonate content of bioapatite [5]; MM index (calculated as the ratio between the intensity of the peaks at 1024 cm^{-1} and 1091 cm^{-1}

associated with apatitic phosphates in well-crystallized stoichiometric hydroxyapatite and in poorly crystalline apatite, respectively) which is related to the mineral maturity [16]; and amide I/PO₄ (calculated as the ratio between the intensity of the peaks at 1639 cm⁻¹ and 1024 cm⁻¹ corresponding respectively to the vibrational modes of the amide I band of proteins and phosphate groups, respectively), which indicates the relative amount of the organic matrix with respect to the inorganic component [3,5]. The numerical variation is reported in Table 2.

Table 2. Diagenetic parameters calculated by ATR-FTIR analysis of human and animal bone samples collected at the Fewet oasis: IRSF, FWHM₆₀₃, C/P, MM, and amide I/PO₄. Data are reported as mean ± S.D.

Sample	IRSF	FWHM ₆₀₃	C/P	MM	AmideI/PO ₄
H-41	2.53 ± 0.226	23.5 ± 0.85	0.136 ± 0.007	2.96 ± 0.11	0.032 ± 0.005
H-669	2.57 ± 0.165	25.1 ± 0.58	0.206 ± 0.005	3.07 ± 0.15	0.087 ± 0.006
H-715	2.46 ± 0.198	24.7 ± 0.60	0.196 ± 0.008	2.56 ± 0.25	0.078 ± 0.004
H-716	3.00 ± 0.225	17.6 ± 0.92	0.043 ± 0.008	3.69 ± 0.22	0.018 ± 0.005
H-914	2.87 ± 0.154	25.6 ± 0.67	0.198 ± 0.007	2.67 ± 0.17	0.058 ± 0.005
H-954	2.38 ± 0.158	24.1 ± 0.56	0.209 ± 0.010	2.88 ± 0.14	0.084 ± 0.005
H-976	2.47 ± 0.151	18.0 ± 0.67	0.105 ± 0.009	2.15 ± 0.14	0.022 ± 0.005
H-1191	2.42 ± 0.215	20.8 ± 0.79	0.135 ± 0.008	2.66 ± 0.19	0.039 ± 0.004
H-1226	2.67 ± 0.169	18.9 ± 0.73	0.174 ± 0.009	3.25 ± 0.17	0.061 ± 0.006
A-2	3.83 ± 0.326	19.7 ± 0.83	0.124 ± 0.008	2.42 ± 0.25	0.053 ± 0.002
A-6	3.40 ± 0.325	18.6 ± 0.95	0.125 ± 0.008	2.37 ± 0.25	0.049 ± 0.002
A-106	3.47 ± 0.201	20.0 ± 1.10	0.149 ± 0.007	2.24 ± 0.25	0.053 ± 0.004

To evaluate differences among groups, the above defined spectral parameters were then submitted to principal component analysis. The PCA scores plot, shown in Figure 3, pinpoints the presence of different spectral populations among groups; in particular, with regards to the human samples, a good segregation was observed along the PC1 axis (61.04% explained variance) between H-716M and H-976M and all the other samples, while PC2 discriminated between male and female bones (16.56% explained variance). Concerning the modern ruminant samples, a good segregation along the PC1 axis was found with respect to most of the human bones, except for H-716M and H-976M, which segregated along the PC2.

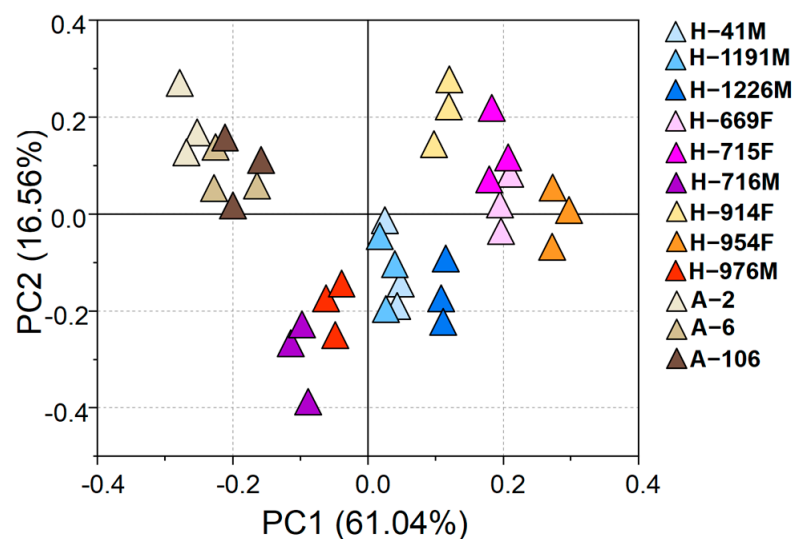


Figure 3. PCA scores plot of bones' spectral parameters; the percentages of variance explained by PC1 and PC2 are reported in brackets.

The statistical analysis of the diagenetic parameters reported in Table 2 is shown in Figure 4. The following considerations can be drawn: (i) with regards to the amide I/ PO_4 ratio, the lowest values were displayed by H-716M and H-976M samples, which also showed the best segregation in the PCA scores plot, whereas samples H-669F, H-715F, and H-954F exhibited the highest ones; (ii) a similar trend was displayed with regards to the C/P index; (iii) concerning the MM index, the highest and lowest values were displayed respectively by samples H-716M and H-976M; (iv) sample H-716M also exhibited the lowest FWHM_{603} and the highest IRSF values; (v) data from the modern ruminants showed intermediate values. All these findings suggest that H-716M and H-976M were characterized by spectral features that were almost different from all the other samples. In particular, in both of these samples, the organic matrix was highly degraded and only a low amount of carbonate ions was present. Moreover, sample H-716M was characterized by a major amount of crystalline hydroxyapatite, as suggested by the low value of FWHM_{603} and by the high values of IRSF and MM.

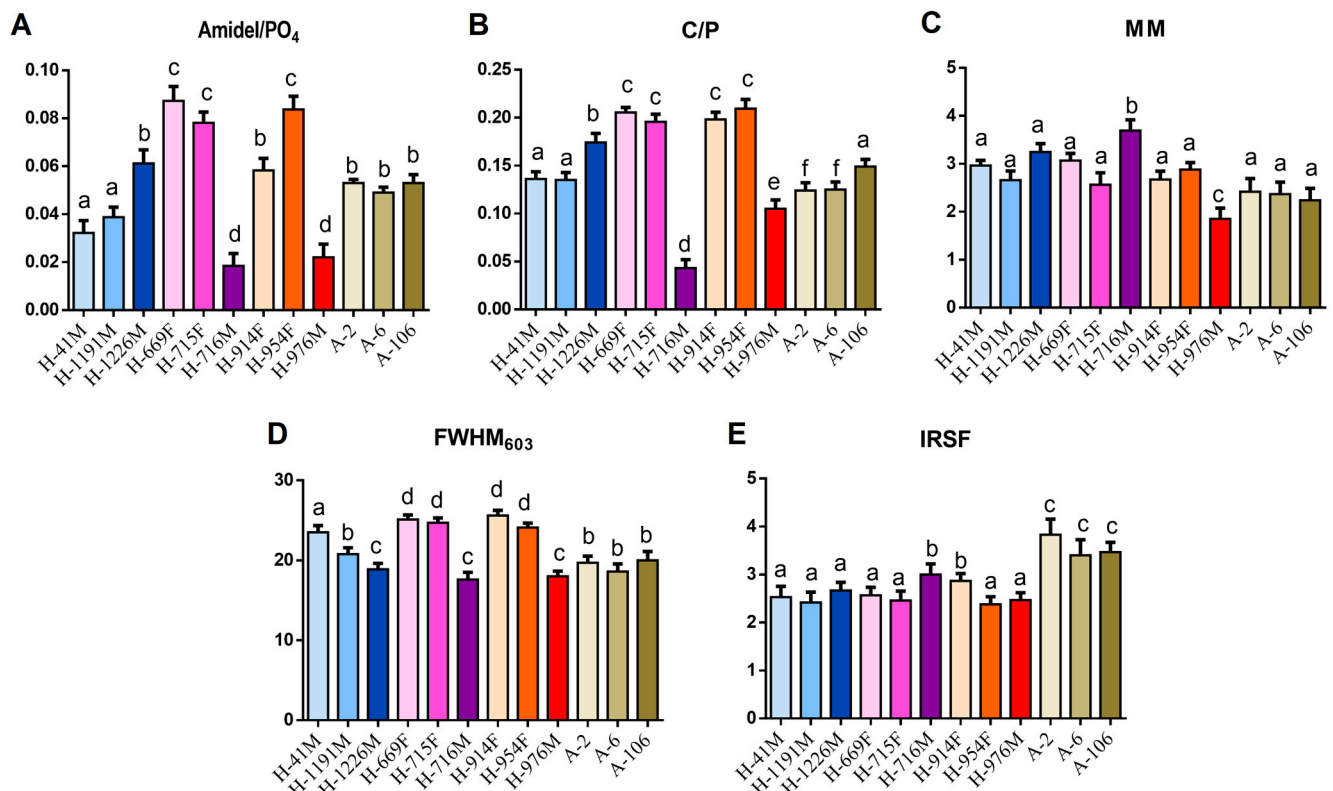


Figure 4. Statistical analysis of the following spectral parameters: (A) Amide I/ PO_4 , (B) C/P, (C) MM, (D) FWHM_{603} , and (E) IRSF. Data are presented as mean \pm SD; different letters indicate statistically significant differences among groups (one-way ANOVA and Tukey's multiple comparison test; $p < 0.05$).

No correlation was found between the C/P and MM indexes among all the groups (Figure 5), which indicated that the level of hydroxyapatite recrystallization of the Fewet samples was independent of their C/P ratio.

Finally, a multinomial logistic regression was performed to investigate the real and numerical correlation between the above defined spectral parameters and specific categorical dependent variables related to humans, such as the presumptive age at death, sex, chronological attribution, and the burial area. A correlation was only found with the burial area (BA1-3 categories for humans and ENV category for animals) (Figure 6). In particular, with regards to the amide I/ PO_4 ratio, the probability associated with BA1 and BA2 reached its maximum level (0.4) at a value of ca. 0.05 of this spectral parameter; the probability of

BA3 displayed an increasing trend, with a maximum of 0.5 at the highest amide I/PO₄ value, while the lowest ones were strongly associated (probability = 1) with the ENV category, hence, to the animal bones. With regards to the C/P ratio, the probability associated with BA1 and BA2 reached the maximum level (0.3) at a value of ca. 0.10 of this spectral parameter, while the probability of BA3 displayed an increasing trend, with a maximum of 0.6 at the highest C/P value; as with the previous case, the C/P lowest values were strongly associated (probability = 0.8) with animal bones. By considering the MM index, the probability associated with BA1, BA3, and ENV showed an almost similar decreasing trend, while the regression line associated with the probability of the BA2 category increased, with a maximum level of almost 0.7 related to the highest MM index values. With regards to the FWHM₆₀₃ value, the probability associated with BA1 showed the highest level of ca. 0.3 with an FWHM₆₀₃ value of 20 and decreased with higher values; the probability associated with BA2 and BA3 showed a superimposable increasing trend, which reached 0.4 with high values of the analyzed spectral feature. Finally, the logistic regression performed by using the IRSF index showed an almost superimposable decreasing trend of probability for BA1, BA2, and BA3 categories, which reached the null probability at >3.25 IRSF values; the highest IRSF values were strongly associated (probability = 1) with animal bones.

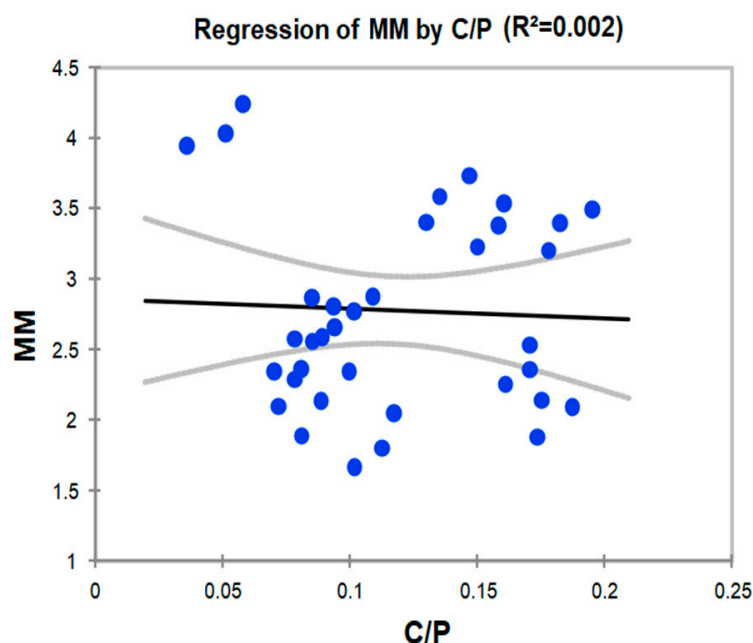


Figure 5. Correlation between C/P and MM indexes calculated for the archaeological human and modern ruminant bones from the Fewet oasis in the Sahara of SW Libya. The central black line represents the regression line of the fitted model; grey lines represent the 95% confidence interval.

Then, the statistical significance of the association between the burial area and the spectral parameters of all samples was determined using the ENV category as the reference (Table 3). No significant effect of the burial area was detected for amide I/PO₄ and MM parameters (significance > 0.05). With regards to the C/P ratio and FWHM₆₀₃, a significant effect was highlighted only for BA2 and BA3 (significance < 0.05), while for the IRSF index, a significant effect was found only for BA1 and BA3 categories (significance < 0.05). Overall, these data confirmed that the chemical and structural features of carbonated hydroxyapatite were different among the samples according to the burial area [5].

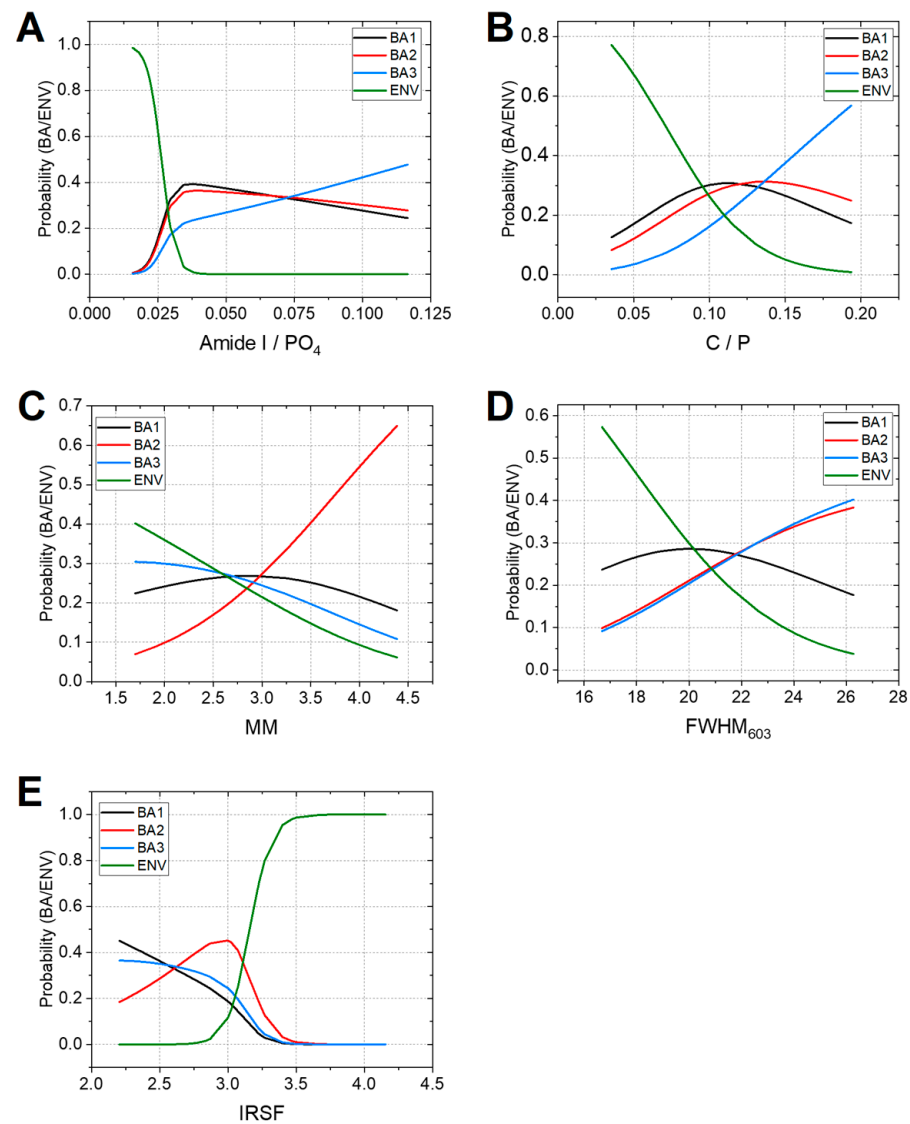


Figure 6. Multinomial logistic regression curves of probability of the burial area (BA1, BA2, and BA3 for the humans and ENV for the modern ruminants), with the following spectral diagenetic parameters: (A) Amide I/PO₄, (B) C/P, (C) MM, (D) FWHM₆₀₃, and (E) IRSF.

Table 3. Results of the multinomial logistic regression analysis performed to assess the association between amide I/PO₄, C/P, MM, FWHM₆₀₃, and IRSF indexes and the burial area. Statistical significance was set at <0.05 and was calculated as the probability of the chi-square test on the log ratio. Significant values are underlined.

	Burial Area	Significance Pr > Chi ²		Burial Area	Significance Pr > Chi ²
Amide I/PO ₄	BA1	0.245	FWHM ₆₀₃	BA1	0.203
	BA2	0.244		BA2	<u>0.037</u>
	BA3	0.239		BA3	<u>0.033</u>
C/P	BA1	0.070	IRSF	BA1	<u>0.033</u>
	BA2	<u>0.040</u>		BA2	0.062
	BA3	<u>0.006</u>		BA3	<u>0.039</u>
MM	BA1	0.424			
	BA2	0.054			
	BA3	0.691			

4. Discussion

Diagenesis is a set of complex postmortem processes which affect both the organic and inorganic components of bones. It begins with death, and potentially extends even to fossilization, causing alterations in the majority of *in vivo* chemical signals of bones [13]. A key role is played by the environmental conditions, but the entity and the complexity of these modifications depend on several factors, including the uptake of cations, ions' exchange, degradation and leaching of collagen, microbiological attack, alteration and, in some cases, leaching of the mineral matrix, infilling with mineral deposits, etc. [4–6]. According to Nielsen–Marsh and Hedge [30], the diagenetic changes in archeological bones are mostly dependent on the burial modality and site. Above all, the driving force of diagenesis is the intra-site hydrology, which appears to have a strong influence on the outcome of bone preservation because of the ionic exchange between the bone and the neighboring burial environment.

It is evident that a careful investigation of all these degradation processes is essential for a reliable reconstruction of the fundamental characteristics of ancient populations, including lifestyle, diet, and provenance [7]. The Garamantian necropolis of the Fewet oasis has been already studied [23–25], but there is a lack of information regarding the diagenetic processes affecting the skeletons buried in this area. Hence, the ATR–FTIR analysis of human bones from this site was carried out in this present study, and the relative information obtained on the chemical and structural composition of the mineral and organic components of these samples appear fundamental to obtain reliable information on these ancient populations.

Useful parameters for the evaluation of archaeological bone diagenesis are the microbial activity damage, the protein content, and changes in bone micro- and macro-porosity [30]. In addition, ATR–FTIR indexes related to the vibrational modes of phosphates and carbonate groups and indicative of the crystallinity of hydroxyapatite (such as the amide I/PO₄, C/P, MM FWHM₆₀₃, and IRSF indexes) were successfully used [3,5,16].

Upon initial evaluation, in all the analyzed bone samples, no peak at 712 cm^{−1} attributable to diagenetic calcite was observed. The absence of or an undetectable content of diagenetic calcite in human bones suggests a very limited circulation of water within the bone-hosting cists, which is also favored by the Saharan hyper-arid climate of the last 2000 years. This is consistent with previous data reported in [5], describing the lack of secondary calcite in archaeological bones, even when Saharan soils were calcite-rich (caliche). Therefore, the absence of diagenetic calcite might be related with the increase of the hydroxyapatite recrystallization rate in bone remains [31]. Moreover, since calcite is more soluble in water than apatite, the potential ion release stabilizes apatite, mainly in the case of a relatively static hydrological regime. This may have accounted for the high FWHM of the peak at 603 cm^{−1} observed in Fewet human bones.

The majority of the Fewet samples displayed C/P values within the range 0.1–0.2, which was lower than the catastrophic bone dissolution (CD) value and closer to the accelerated collagen loss (ACL) value [32], which leads us to hypothesize that these processes were likely those mainly responsible for bone diagenesis. Moreover, the comparison between the C/P values of Fewet bone samples and those of the modern analogs (C/P > 0.67) suggests a low carbonate exchange in the former [3,5]. Lacking any correlation between the C/P and MM indexes, the absence of diagenetic calcite could be ascribable to the input of soil carbonates into the crystalline lattice of the bone [30,33]. Given that the C/P values of samples H-716M and H-976M were similar to those of modern ruminant bones, this may be explained by either a loss of carbonate or a higher rate of hydroxyapatite recrystallization.

In general, except for the H-716M and H-976M samples, Fewet human bones displayed a high preservation of the organic matrix, as shown by the values of the amide I/PO₄ ratio, which were higher than those found in modern ruminant bones. Significantly lower values of the FWHM₆₀₃ index were observed in Fewet samples (human and animal ones) with respect to fresh human and animal bones [5,31,32], which indicated a rather variable rate of diagenesis. With regards to the IRSF index, Fewet human bone samples

displayed lower values with respect to those found in the modern ruminant bones from the same area and, in general, with respect to modern human and animal bones [3]; IRSF Fewet values were also far from those of bones affected by CD (>3.5) and ACL (>4.0) values, which suggested a mild diagenesis [32].

Moreover, the multinomial logistic regression showed a numerical correlation between the chemical bone composition of the bones and their burial sites; interestingly, no correlation existed between bones spectral features and death age, sex, chronological attribution of the individuals, or environmental conditions [4,5].

The comparison between the ATR–FTIR data of Fewet human bones and those belonging to Meroitic individuals collected from the Al-Khiday multi-layered cemetery (Sudan) provided further information on diagenesis [5]; interestingly, these humans lived under climatic (Saharan hyper-arid) and chronological (800 B.C.–350 A.D.) features similar to those of Fewet humans, but they were subjected to significantly different burial conditions; at Al-Khiday, bones were inhumated, whereas at Fewet, they were placed in cists. Therefore, inhumation might explain why Al-Khiday bones displayed comparatively higher (0.09–0.14) values of the C/P ratio as well as of the FWHM₆₀₃ (44.4–66.2) and IRSF (5.4–6.2) indexes [5], likely because significant ion exchanges between bones and the soil solution occurred there. In turn, this may support that Fewet bones underwent mild diagenesis.

As a whole, the FWHM₆₀₃, C/P, and MM indexes of ATR–FTIR data made it possible to distinguish between modern and archeological human bones. Moreover, the comparison between Fewet and Al-Khiday bone samples, which were similar in age, geological substrate, and climatic condition, but different in the burial style, suggests that bone recrystallization processes are strongly susceptible to the influence of external diagenetic factors.

5. Conclusions

ATR–FTIR spectroscopy was successfully applied to study human bone samples from several burials of the Garamantian necropolis of the Fewet oasis in SW Libya. Spectral results suggest that the analyzed bone samples underwent mild diagenesis, which was confirmed by comparing the data with analogs of modern ruminant bones from the same area. In particular, human bones underwent a higher rate of carbonate loss relative to phosphate loss and were degraded mainly because of a loss of proteins and collagen. Among all the bones studied, samples H-716M and H-976M were more affected by diagenesis, as they were the most recrystallized, and showed the lowest amounts of organic components (amide I/PO₄ ratio), carbonate groups relative to phosphates (A₁₄₁₂/A₁₀₂₄ ratio), and FWHM₆₀₃ indexes. Moreover, sample H-716M shows the highest MM (A₁₀₂₄/A₁₀₉₁ ratio) value.

Interestingly, a correlation was found with the burial site. In fact, the samples from the BA1 location showed low values of the IRSF index, whereas those from the BA2 location displayed high values of the A₁₀₂₄/A₁₀₉₁ ratio, the FWHM₆₀₃, and IRSF indexes, and, lastly, the samples from the BA3 location exhibited high values of the A₁₄₁₂/A₁₀₂₄ ratio and the FWHM₆₀₃ index. The relationship between most of the IR data of the human bones and burial areas showed that the bones from the lower levels of the necropolis generally exhibited a higher rate of hydroxyapatite recrystallization, i.e., a higher diagenetic impact. Moreover, the human bones displayed lower amounts of organic matter relative to phosphates and IRSF values. The FWHM₆₀₃ and MM indexes, along with the C/P ratios, did not distinguish between the human and modern ruminant bones, which suggested that both underwent early diagenesis. In contrast, the lower IRSF values of the human bones made it possible to distinguish them from those of modern ruminants.

Lastly, the comparison of the IR data of cist-posed Fewet human bones with those of coeval Meroitic individuals from the Al-Khiday (Sudan) cemetery, who lived under similar climatic conditions but were inhumated after death, showed different patterns of bone diagenesis. In fact, Fewet bones displayed comparatively lower values of the IRSF, FWHM₆₀₃, and C/P ratios, likely because of the lack of significant ion exchange between the bone and the soil.

Author Contributions: Conceptualization, F.C. and U.M.; formal analysis, E.G. and V.N.; resources, L.M. and M.A.T.; data curation, V.N.; writing—original draft preparation, F.C., E.G. and V.N.; writing—review and editing, F.C., E.G. and V.N. All authors have read and agreed to the published version of the manuscript.

Funding: This work was supported by Università di Roma “La Sapienza”, grants project “Grandi Scavi” through Prof. Savino Di Lernia.

Data Availability Statement: Not applicable.

Acknowledgments: We thank Carla Conti for her precious support in ATR spectra collection.

Conflicts of Interest: The authors declare no conflict of interest.

References

1. Ferretti, A.; Medici, L.; Savioli, M.; Mascia, M.T.; Malferrari, D. Dead, fossil or alive: Bioapatite diagenesis and fossilization. *Palaeogeogr. Palaeoclimatol. Palaeoecol.* **2021**, *579*, 110608. [[CrossRef](#)]
2. Surmik, D.; Boczarowski, A.; Balin, K.; Dulski, M.; Szade, J.; Kremer, B.; Pawlicki, R. Spectroscopic Studies on Organic Matter from Triassic Reptile Bones, Upper Silesia, Poland. *PLoS ONE* **2016**, *11*, e0151143. [[CrossRef](#)] [[PubMed](#)]
3. Dal Sasso, G.; Asscher, Y.; Angelini, I.; Nodari, L.; Artioli, G. A universal curve of apatite crystallinity for the assessment of bone integrity and preservation. *Sci. Rep.* **2018**, *8*, 12025. [[CrossRef](#)] [[PubMed](#)]
4. Hedges, R.E.M. Bone diagenesis: An overview of processes. *Archaeometry* **2002**, *44*, 319–328. [[CrossRef](#)]
5. Dal Sasso, G.; Lebon, M.; Angelini, I.; Maritan, L.; Usai, D.; Artioli, G. Bone diagenesis variability among multiple burial phases at Al Khiday (Sudan) investigated by ATR–FTIR spectroscopy. *Palaeogeogr. Palaeoclimatol. Palaeoecol.* **2016**, *463*, 168–179. [[CrossRef](#)]
6. Kontopoulos, I.; Penkman, K.; Liritzis, I.; Collins, M.J. Bone diagenesis in a Mycenaean secondary burial (Kastrouli, Greece). *Archaeol. Anthropol. Sci.* **2019**, *11*, 5213–5230. [[CrossRef](#)]
7. Rasmussen, K.L.; Milner, G.; Skytte, L.; Lynnerup, N.; Thomsen, J.L.; Boldsen, J.L. Mapping diagenesis in archaeological human bones. *Herit. Sci.* **2019**, *7*, 41. [[CrossRef](#)]
8. Kendall, C.; Eriksen, A.M.H.; Kontopoulos, I.; Collins, M.J.; Turner-Walker, G. Diagenesis of archaeological bone and tooth. *Palaeogeogr. Palaeoclimatol. Palaeoecol.* **2018**, *491*, 21–37. [[CrossRef](#)]
9. Arthur Augusto de Castro, P.; Augusto Dias, D.; Del-Valle, M.; Noronha Veloso, M.; Sebastiana Ribeiro Somessari, E.; Maria Zzell, D. Assessment of bone dose response using ATR–FTIR spectroscopy: A potential method for biodosimetry. *Spectrochim. Acta Part A Mol. Biomol. Spectrosc.* **2022**, *273*, 120900. [[CrossRef](#)]
10. Martínez Cortizas, A.; López-Costas, O. Linking structural and compositional changes in archaeological human bone collagen: An FTIR-ATR approach. *Sci. Rep.* **2020**, *10*, 17888. [[CrossRef](#)]
11. France, C.A.M.; Sugiyama, N.; Aguayo, E. Establishing a preservation index for bone, dentin, and enamel bioapatite mineral using ATR–FTIR. *J. Archaeol. Sci. Rep.* **2020**, *33*, 102551. [[CrossRef](#)]
12. Orilisi, G.; Tosco, V.; Monterubbianesi, R.; Notarstefano, V.; Özcan, M.; Putignano, A.; Orsini, G. ATR–FTIR, EDS and SEM evaluations of enamel structure after treatment with hydrogen peroxide bleaching agents loaded with nano-hydroxyapatite particles. *PeerJ* **2021**, *9*, e10606. [[CrossRef](#)] [[PubMed](#)]
13. Kasem, M.A.; Yousef, I.; Alrowaili, Z.A.; Zedan, M.; El-Husseini, A. Investigating Egyptian archeological bone diagenesis using ATR–FTIR microspectroscopy. *J. Radiat. Res. Appl. Sci.* **2020**, *13*, 515–527. [[CrossRef](#)]
14. Mudunkotuwa, I.A.; Minshid, A.A.; Grassian, V.H. ATR–FTIR spectroscopy as a tool to probe surface adsorption on nanoparticles at the liquid–solid interface in environmentally and biologically relevant media. *Analyst* **2014**, *139*, 870–881. [[CrossRef](#)]
15. Henderson, E.J.; Helwig, K.; Read, S.; Rosendahl, S.M. Infrared chemical mapping of degradation products in cross-sections from paintings and painted objects. *Herit. Sci.* **2019**, *7*, 71. [[CrossRef](#)]
16. Farlay, D.; Panczer, G.; Rey, C.; Delmas, P.D.; Boivin, G. Mineral maturity and crystallinity index are distinct characteristics of bone mineral. *J. Bone Miner. Metab.* **2010**, *28*, 433–445. [[CrossRef](#)]
17. Kontopoulos, I.; Presslee, S.; Penkman, K.; Collins, M.J. Preparation of bone powder for FTIR-ATR analysis: The particle size effect. *Vib. Spectrosc.* **2018**, *99*, 167–177. [[CrossRef](#)]
18. Cremaschi, M.; Zerboni, A. Early to Middle Holocene landscape exploitation in a drying environment: Two case studies compared from the central Sahara (SW Fezzan, Libya). *Comptes Rendus Geosci.* **2009**, *341*, 689–702. [[CrossRef](#)]
19. Zerboni, A.; Perego, A.; Cremaschi, M. Geomorphological Map of the Tadrart Acacus Massif and the Erg Uan Kasa (Libyan Central Sahara). *J. Maps* **2015**, *11*, 772–787. [[CrossRef](#)]
20. Mori, L. (Ed.) *Life and Death of a Rural Village in Garamantian Times: Archaeological Investigations in the Oasis of Fewet (Libyan Sahara)*; New York University: New York, NY, USA, 2013.
21. Ricci, F.; Tafuri, M.A.; Di Vincenzo, F.; Manzi, G. The human skeletal sample from Fewet. In *Life and Death of A Rural Village in Garamantian Times: Archaeological Investigations in the Oasis of Fewet (Libyan Sahara)*.—(Arid Zone Archaeology Monographs 2035-5459; 6); All’Insegna del Giglio: Firenze, Italy, 2013; ISBN 9788878145948.
22. Hallett, D.; Clark-Lowes, D. *Petroleum Geology of Libya*; Elsevier: Amsterdam, The Netherlands, 2017; ISBN 978-0-444-63517-4.

23. Liverani, M.; Barbato, L.; Cancellieri, E.; Castelli, R.; Putzolu, C. The survey of the Fewet necropolis. In *Life and Death of A Rural Village in Garamantian Times: Archaeological Investigations in the Oasis of Fewet (Libyan Sahara)*.—(Arid zone Archaeology Monographs 2035-5459; 6); All'Insegna del Giglio: Firenze, Italy, 2013; ISBN 9788878145948.
24. Mori, L.; Ricci, F.; Gatto, M.C.; Cancellieri, E.; Lemorini, C. The excavation of the Fewet necropolis. In *Life and Death of A Rural Village in Garamantian Times: Archaeological Investigations in the Oasis of Fewet (Libyan Sahara)*.—(Arid Zone Archaeology Monographs 2035-5459; 6); All'Insegna del Giglio: Firenze, Italy, 2013; ISBN 9788878145948.
25. di Lernia, S.; Tafuri, M.A. Persistent deathplaces and mobile landmarks: The Holocene mortuary and isotopic record from Wadi Takarkori (SW Libya). *J. Anthropol. Archaeol.* **2013**, *32*, 1–15. [[CrossRef](#)]
26. Tafuri, M.A.; Pelosi, A.; Ricci, F.; Manzi, G.; Castorina, F. The preliminary isotope investigation. In *Life and Death of A Rural Village in Garamantian Times: Archaeological Investigations in the Oasis of Fewet (Libyan Sahara)*.—(Arid Zone Archaeology Monographs 2035-5459; 6); All'Insegna del Giglio: Firenze, Italy, 2013; ISBN 9788878145948.
27. Notarstefano, V.; Sabbatini, S.; Pro, C.; Belloni, A.; Orilisi, G.; Rubini, C.; Byrne, H.J.; Vaccari, L.; Giorgini, E. Exploiting fourier transform infrared and Raman microspectroscopies on cancer stem cells from oral squamous cells carcinoma: New evidence of acquired cisplatin chemoresistance. *Analyst* **2020**, *145*, 8038–8049. [[CrossRef](#)]
28. Notarstefano, V.; Belloni, A.; Sabbatini, S.; Pro, C.; Orilisi, G.; Monterubbianesi, R.; Tosco, V.; Byrne, H.J.; Vaccari, L.; Giorgini, E. Cytotoxic Effects of 5-Azacytidine on Primary Tumour Cells and Cancer Stem Cells from Oral Squamous Cell Carcinoma: An In Vitro FTIRM Analysis. *Cells* **2021**, *10*, 2127. [[CrossRef](#)]
29. Weiner, S.; Bar-Yosef, O. States of preservation of bones from prehistoric sites in the Near East: A survey. *J. Archaeol. Sci.* **1990**, *17*, 187–196. [[CrossRef](#)]
30. Nielsen-Marsh, C.M.; Hedges, R.E. Patterns of Diagenesis in Bone I: The Effects of Site Environments. *J. Archaeol. Sci.* **2000**, *27*, 1139–1150. [[CrossRef](#)]
31. Berna, F.; Matthews, A.; Weiner, S. Solubilities of bone mineral from archaeological sites: The recrystallization window. *J. Archaeol. Sci.* **2004**, *31*, 867–882. [[CrossRef](#)]
32. Smith, C.I.; Nielsen-Marsh, C.M.; Jans, M.M.E.; Collins, M.J. Bone diagenesis in the European Holocene I: Patterns and mechanisms. *J. Archaeol. Sci.* **2007**, *34*, 1485–1493. [[CrossRef](#)]
33. Szostek, K.; Stepańczyk, B.; Szczepanek, A.; Kępa, M.; Głąb, H.; Jarosz, P.; Włodarczyk, P.; Tunia, K.; Pawlyta, J.; Paluszkiwicz, C.; et al. Diagenetic signals from ancient human remains—Bioarchaeological applications. *Mineralogia* **2011**, *42*, 93–112. [[CrossRef](#)]

Disclaimer/Publisher's Note: The statements, opinions and data contained in all publications are solely those of the individual author(s) and contributor(s) and not of MDPI and/or the editor(s). MDPI and/or the editor(s) disclaim responsibility for any injury to people or property resulting from any ideas, methods, instructions or products referred to in the content.